Thermochimica Acta 498 (2010) 22–26

Contents lists available at ScienceDirect

Thermochimica Acta

journal homepage: www.elsevier.com/locate/tca

Thermodynamic assessment of Ag–Dy–Sb ternary system

Z.H. Long, S.X. Zhou, H.S. Liu*, Z.P. Jin

School of Materials Science and Engineering, Central South University, Changsha, Hunan Province, 410083, PR China

ARTICLE INFO

Article history:
Received 4 August 2009
Accepted 17 September 2009
Available online 23 September 2009

Keywords:
Dy–Sb binary system
Ag–Dy–Sb ternary system
Thermodynamic modeling
CALPHAD method

ABSTRACT

Thermodynamic description of the Ag–Dy–Sb ternary system has been performed. At first, the boundary binary Dy–Sb system has been thermodynamically assessed with CALPHAD method. The solution phases including liquid, Bcc and Hcp were described with a substitutional model, of which the excess Gibbs energies were formulated with the Redlich–Kister polynomial. All the binary intermetallic phases, i.e. Dy_5Sb_3, Dy_4Sb_3 and DySb, were treated as stoichiometric compounds. Then, combined with the thermodynamic parameters of the Ag–Dy and Ag–Sb binary systems cited from literatures, the Ag–Dy–Sb ternary system was thermodynamically assessed. The calculated phase equilibria were in good agreement with the reported experimental data.

1. Introduction

Silver with high electronic-conductivity has found wide application in electronic industry. However, pure Ag is of poor strength and cannot withstand high temperature. Fortunately, addition of antimony and rare earth elements into Ag can enhance its strength [1–2]. Besides, the melting points of many Ag-RE intermetallic compounds are very high. These compounds can improve the stability of Ag-base alloy at high temperature [2]. In order to provide useful information for develop new materials to satisfy new usages, phase diagrams of the Ag-related system are necessary. In this work, the Ag–Dy–Sb ternary system is assessed through CALPHAD approach.

2. Experiment information

2.1. The Dy–Sb binary system

Mironov et al. [3] have constructed phase diagram of the Dy–Sb system by using thermal analysis, X-ray diffraction and microstructure observation. Three compounds, Dy_5Sb_3, Dy_4Sb_3 and DySb, have been detected. Among these compounds, Dy_5Sb_3 and Dy_4Sb_3 form through peritectic reactions at 1953 K and 2053 K, respectively, whereas DySb melts congruently at 2443 K.

According to Mironov et al. [3], Dy_4Sb_3 could be stable from 2053 K down to room temperature. However, this result may be dubious according to the later studies [2,4–7]. On the basis of the experimental investigations [2,4–7], Dy_4Sb_3 decomposes eutectoidly into Dy_5Sb_3 and DySb at low temperature. Especially, Morozkin's experimental result [4] indicated that Dy_4Sb_3 was unstable at 1100 K. So, the eutectoid temperature is above 1100 K. Experimental information in Refs. [2,4–7] may be more reliable and is given higher weight in the present assessment.

Besides, Mironov et al. [3] indicated that the liquidus in the region of compositions with more than 50 at.% Sb was difficult to be measured reliably because of the high volatility of Sb at high temperature. So, lower weight has been given to the liquidus in the region of compositions with more than 50 at.% Sb during assessment.

As for thermodynamic properties, only the formation enthalpies of the three compounds, i.e. Dy_5Sb_3, Dy_4Sb_3 and DySb, were reported. By calorimetric measurement along with X-ray diffraction and metallographic analyses, Ferro et al. [8] measured the formation enthalpies of Dy_5Sb_3, Dy_4Sb_3 and DySb at 300 K. These thermodynamic data will be adopted in the present optimization.

2.2. The Ag–Dy and Ag–Sb binary systems

The Ag–Dy binary system has recently been assessed by Long et al. (unpublished work). The assessed phase diagram of Ag–Dy was shown in Fig. 1. Their thermodynamic parameters can reproduce most experimental phase diagram and thermodynamic properties well. Hence, the parameters assessed by Long et al. were directly adopted in present work.

Thermodynamic assessment of the Ag–Sb system had been carried out by Lee et al. [9]. However, their parameters could not well reproduce the experimental phase diagram in the temperature range below 500 K, and the calculated heats of formation of the solid phases showed large discrepancies from the experimental ones. Later, Oh et al. [10] reassessed this binary system, and most experimental data including the phase diagram at low temperature

* Corresponding author. Tel.: +86 073188876735; fax: +86 073188876692.
E-mail address: hsliu@mail.csu.edu.cn (H.S. Liu).

0040-6031/$ – see front matter © 2009 Elsevier B.V. All rights reserved.
doi:10.1016/j.tca.2009.09.006

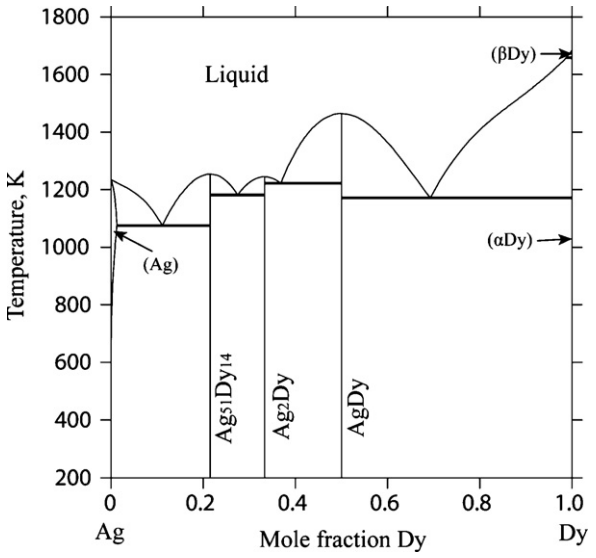

Fig. 1. The calculated Ag–Dy phase diagram by Long et al.

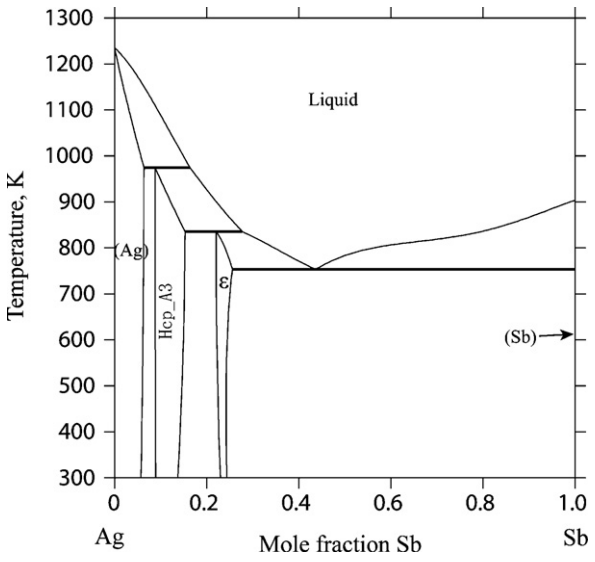

Fig. 2. The calculated Ag–Sb phase diagram [10].

Table 1
Optimized parameters of Ag–Dy–Sb ternary system.

Phase	Thermodynamic parameters	References
Liquid	${}^{0}L^{Liq}_{Ag,Dy} = -120,882.06 + 21.174T$	Long et al.
	${}^{1}L^{Liq}_{Ag,Dy} = -69,962.11 + 27.008T$	Long et al.
	${}^{2}L^{Liq}_{Ag,Dy} = 27{,}773.12$	Long et al.
	${}^{3}L^{Liq}_{Ag,Dy} = 18,181.39$	Long et al.
	${}^{0}L^{Liq}_{Ag,Sb} = -821.8 - 9.656T$	[10]
	${}^{1}L^{Liq}_{Ag,Sb} = -19,309 + 4.424T$	[10]
	${}^{2}L^{Liq}_{Ag,Sb} = -10,381.2$	[10]
	${}^{0}L^{Liq}_{Dy,Sb} = -272,808.51 - 24.975T$	This work
	${}^{1}L^{Liq}_{Dy,Sb} = 16,379.60 - 12.158T$	This work
	${}^{2}L^{Liq}_{Dy,Sb} = 88,463.43$	This work
Fcc	${}^{0}L^{Fcc}_{Ag,Dy} = -65,136.13 - 5.743T$	Long et al.
	${}^{0}L^{Fcc}_{Ag,Sb} = -22,937.9 + 54.185T$	[10]
	${}^{1}L^{Fcc}_{Ag,Sb} = -530.7 - 58.387T$	[10]
Bcc	${}^{0}L^{Bcc}_{Dy,Sb} = -210,000$	This work
Hcp	${}^{0}L^{Hcp}_{Ag,Dy} = 100,000$	Long et al.
	${}^{0}L^{Hcp}_{Ag,Sb} = -23,050.3 + 38.368T$	[10]
	${}^{1}L^{Hcp}_{Ag,Sb} = -5357.5 - 45.064T$	[10]
	${}^{0}L^{Hcp}_{Dy,Sb} = -200,000$	This work
$Ag_{51}Dy_{14}$	${}^{0}G^{Ag_{51}Dy_{14}}_{Ag:Dy} = 0.7846\,{}^{0}G^{Fcc}_{Ag} + 0.2154\,{}^{0}G^{Hcp}_{Dy} - 23939.75 + 1.445T$	Long et al.
Ag_2Dy	${}^{0}G^{Ag_2Dy}_{Ag:Dy} = 0.6667\,{}^{0}G^{Fcc}_{Ag} + 0.3333\,{}^{0}G^{Hcp}_{Dy} - 31050 + 2.207T$	Long et al.
AgDy	${}^{0}G^{AgDy}_{Ag:Dy} = 0.5\,{}^{0}G^{Fcc}_{Ag} + 0.5\,{}^{0}G^{Hcp}_{Dy} - 35,003.2 + 2.704T$	Long et al.
ε	${}^{0}G^{Ortho}_{Ag:Ag} = {}^{0}G^{Fcc}_{Ag} + 4750 - 0.5T$	[10]
	${}^{0}G^{Ortho}_{Ag:Sb} = 0.75\,{}^{0}G^{Fcc}_{Ag} + 0.25\,{}^{0}G^{Rho}_{Sb} - 338.5 - 4.5184T$	[10]
	${}^{0}G^{Ortho}_{Sb:Ag} = 0.25\,{}^{0}G^{Fcc}_{Ag} + 0.75\,{}^{0}G^{Rho}_{Sb} + 23,223.9$	[10]
	${}^{0}G^{Ortho}_{Sb:Sb} = {}^{0}G^{Rho}_{Sb} + 20,000 - 10T$	[10]
	${}^{0}L^{Ortho}_{Ag:(Ag,Sb)} = -4873.3$	[10]
	${}^{0}L^{Ortho}_{(Ag,Sb):Sb} = +5932.3$	[10]
Dy_5Sb_3	${}^{0}G^{Dy_5Sb_3}_{Dy:Sb} = 0.625\,{}^{0}G^{Hcp}_{Dy} + 0.375\,{}^{0}G^{Rho}_{Sb} - 99,569.55 + 1.266T$	This work
β_Dy_4Sb_3	${}^{0}G^{Dy_4Sb_3\_H}_{Dy:Sb} = 0.5714\,{}^{0}G^{Hcp}_{Dy} + 0.4286\,{}^{0}G^{Rho}_{Sb} - 106,742.07 + 0.039T$	This work
α_Dy_4Sb_3	${}^{0}G^{Dy_4Sb_3\_L}_{Dy:Sb} = 0.5714\,{}^{0}G^{Hcp}_{Dy} + 0.4286\,{}^{0}G^{Rho}_{Sb} - 107,715 + 0.55T$	This work
β_DySb	${}^{0}G^{DySb\_H}_{Dy:Sb} = 0.5\,{}^{0}G^{Hcp}_{Dy} + 0.5\,{}^{0}G^{Rho}_{Sb} - 117,655.46 + 0.035T$	This work
α_DySb	${}^{0}G^{DySb\_L}_{Dy:Sb} = 0.5\,{}^{0}G^{Hcp}_{Dy} + 0.5\,{}^{0}G^{Rho}_{Sb} - 120,496.2 + 1.3486T$	This work
τ_1	${}^{0}G^{\tau_1}_{Ag:Dy:Sb} = 0.38462\,{}^{0}G^{Fcc}_{Ag} + 0.53846\,{}^{0}G^{Hcp}_{Dy} + 0.07692\,{}^{0}G^{Rho}_{Sb} - 48,000$	This work
τ_2	${}^{0}G^{\tau_2}_{Ag:Dy:Sb} = 0.25\,{}^{0}G^{Fcc}_{Ag} + 0.25\,{}^{0}G^{Hcp}_{Dy} + 0.5\,{}^{0}G^{Rho}_{Sb} - 62,250$	This work

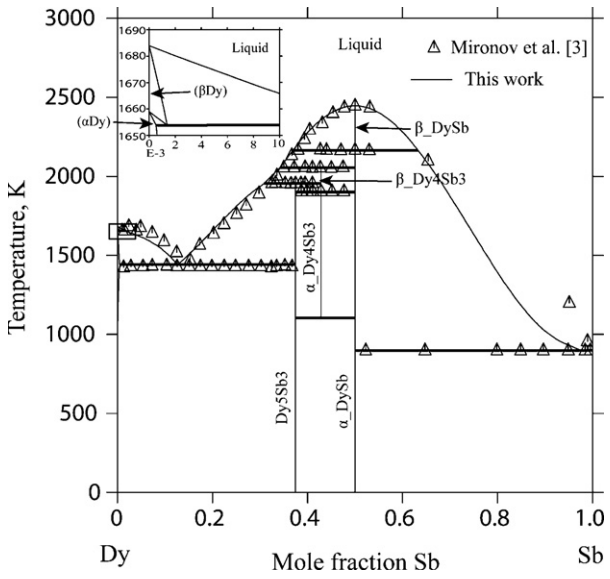

Fig. 3. The calculated Dy–Sb phase diagram with the experimental data [3].

and heats of formation of the solid phases were well reproduced. So, the thermodynamic parameters reported by Oh et al. [10] were adopted in this work. Fig. 2 illustrates the calculated phase diagram based on Oh et al.'s assessment.

2.3. The Ag–Dy–Sb ternary system

Zeng and Xie [7] has established the isothermal section of this ternary system at 673 K by powder X-ray diffraction with the aid of optical microscopy and scanning electron microscopy. Two ternary compounds, i.e. Ag_5Dy_7Sb and $AgDySb_2$, were detected and their crystal structures determined. No remarkable solubility of the third element in the binary phases was detected.

3. Thermodynamic model

3.1. Solution phases

A substitutional solution model based on random mixing of the constituent atoms is employed to describe liquid, Bcc, Fcc and Hcp solutions. The molar Gibbs energy of a solution phase Φ (Φ = liquid, Bcc, Fcc, Hcp) is expressed as:

$$G^{\Phi} = \sum_{i=\mathrm{Ag,Dy,Sb}} x_i^0 G_i^{\Phi} + RT \sum_{i=\mathrm{Ag,Dy,Sb}} x_i \ln x_i + {}^{E}G_m^{\Phi} \tag{1}$$

where

$$\begin{aligned} {}^{E}G_m^{\Phi} = {} & x_{\mathrm{Ag}}x_{\mathrm{Dy}} \sum_{j=0,1,\ldots}^{N} (x_{\mathrm{Ag}} - x_{\mathrm{Dy}})^{j(j)} L_{\mathrm{Ag,Dy}}^{\Phi} + x_{\mathrm{Dy}}x_{\mathrm{Sb}} \\ & \sum_{j=0,1,\ldots}^{N} (x_{\mathrm{Dy}} - x_{\mathrm{Sb}})^{j(j)} L_{\mathrm{Dy,Sb}}^{\Phi} + x_{\mathrm{Ag}}x_{\mathrm{Sb}} \\ & \sum_{j=0,1,\ldots}^{N} (x_{\mathrm{Ag}} - x_{\mathrm{Sb}})^{j(j)} L_{\mathrm{Ag,Sb}}^{\Phi} + x_{\mathrm{Ag}}x_{\mathrm{Dy}}x_{\mathrm{Sb}} L_{\mathrm{Ag,Dy,Sb}}^{\Phi} \end{aligned} \tag{2}$$

here Φ denotes the solution phases, x_i (i = Ag, Dy and Sb) means mole fraction of component i, and ${}^{0}G_i^{\Phi}$ is the molar Gibbs energy of pure element i in the structural state of Φ. ${}^{(j)}L_{\mathrm{Ag,Dy}}^{\Phi}$ is taken from Long et al. and ${}^{(j)}L_{\mathrm{Ag,Sb}}^{\Phi}$ from Oh et al. [10]. ${}^{(j)}L_{\mathrm{Dy,Sb}}^{\Phi}$ is expressed as:

$${}^{(j)}L_{\mathrm{Dy,Sb}}^{\Phi} = A_j + B_j T \tag{3}$$

where A_j and B_j are constants to be optimized. $L_{\mathrm{Ag,Dy,Sb}}^{\Phi}$ is the ternary interaction parameter and set to zero due to lack of experimental data.

Table 2
Comparison of invariant reactions in the Dy–Sb system.

Reaction	Composition of liquid (X_{Sb})	T (K)	Type	References
L ↔ Hcp(Dy) + Dy_5Sb_3	0.126	1441	Eutectic	This work
	0.145	1433	Eutectic	[3]
L ↔ α_DySb + Rho	0.975	898	Eutectic	This work
	0.99	895	Eutectic	[3]
L + Bcc(Dy) ↔ Hcp(Dy)	0.018	1654	Peritectic	This work
	0.075	1653	Peritectic	[3]
L + β_Dy_4Sb_3 ↔ Dy_5Sb_3	0.309	1953	Peritectic	This work
	0.325	1953	Peritectic	[3]
L + α_DySb ↔ β_Dy_4Sb_3	0.342	2053	Peritectic	This work
	0.35	2053	Peritectic	[3]
L + β_DySb ↔ α_DySb	0.369	2163	Peritectic	This work
	0.38	2163	Peritectic	[3]
L + β_DySb ↔ α_DySb	0.632	2163	Peritectic	This work
	0.63	2163	Peritectic	[3]
L ↔ β_DySb	0.5	2445	Congruent	This work
	0.5	2443	Congruent	[3]
β_Dy_4Sb_3 ↔ α_Dy_4Sb_3	–	1900	Allotropic	This work
	–	1903	Allotropic	[3]
β_DySb ↔ α_DySb	–	2163	Allotropic	This work
	–	2163	Allotropic	[3]
α_Dy_4Sb_3 ↔ Dy_5Sb_3 + α_DySb	–	1103	Eutectoidal	This work
	–	>1100	Eutectoidal	[4]

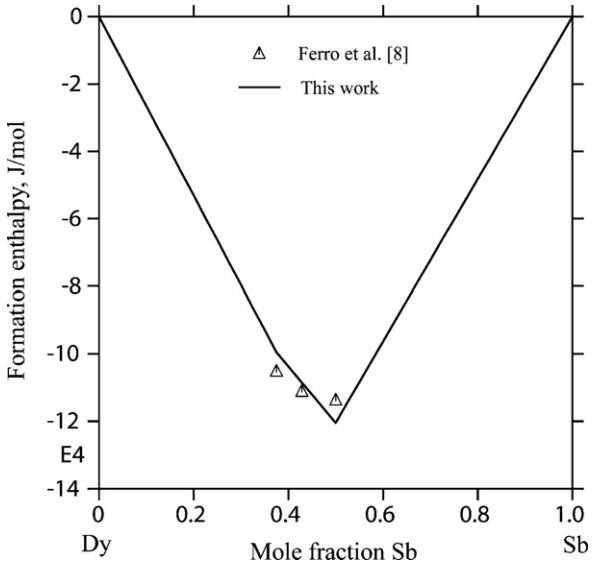

Fig. 4. Calculated formation enthalpies of the compounds compared with experimental data [8]. Reference states: Hcp_A3 Dy and Rhombohedral_A7 Sb.

3.2. Binary intermetallic compounds

All the binary intermetallic phases except ε in the Ag–Sb system are treated as stoichiometric phases, which are described as M_pN_q. Because the experimental data on heat capacity is unavailable, the Gibbs energy of the phase M_pN_q is simply formulated by using Neumann–Kopp rule as:

$$G_{M_pN_q} = \frac{p}{p+q}{}^0G_M^{\mathrm{HSER}} + \frac{q}{p+q}{}^0G_N^{\mathrm{HSER}} + A + BT \quad (4)$$

where M and N denote Ag, Dy or Sb, A and B are the adjusted parameters.

The intermediate phase ε in the Ag–Sb system has an orthorhombic structure with a β-Cu_3Ti prototype, which exhibits a rather wide range of homogeneity. Gibbs energy of this phase is directly taken from Oh et al. [10].

3.3. Ternary intermetallic compounds

There is no report about the homogeneity range of the ternary phases. So, τ_1-Ag_5Dy_7Sb and τ_2-$AgDySb_2$ are modeled as stoichiometric phases, $Ag_xDy_ySb_z$, of which the Gibbs energy are modeled as following:

$$G_{\mathrm{Ag_xDy_ySb_z}} = \frac{x}{x+y+z}{}^0G_{\mathrm{Ag}}^{\mathrm{Fcc}} + \frac{y}{x+y+z}{}^0G_{\mathrm{Dy}}^{\mathrm{Hcp}} + \frac{z}{x+y+z}{}^0G_{\mathrm{Sb}}^{\mathrm{Rho}} + C + DT \quad (5)$$

here C and D are the parameters to be optimized in this work.

4. Results and discussion

4.1. The Dy–Sb binary system

With the lattice stabilities cited from Dinsdale [11], thermodynamic assessment of the Dy–Sb system was carried out by using the Thermo_Calc program and the parameters were listed in Table 1, which reproduce most experimental data well as can be seen in the next paragraphs.

Fig. 3 shows the calculated phase diagram of the Dy–Sb system compared with experimental data [3], and the invariant reactions

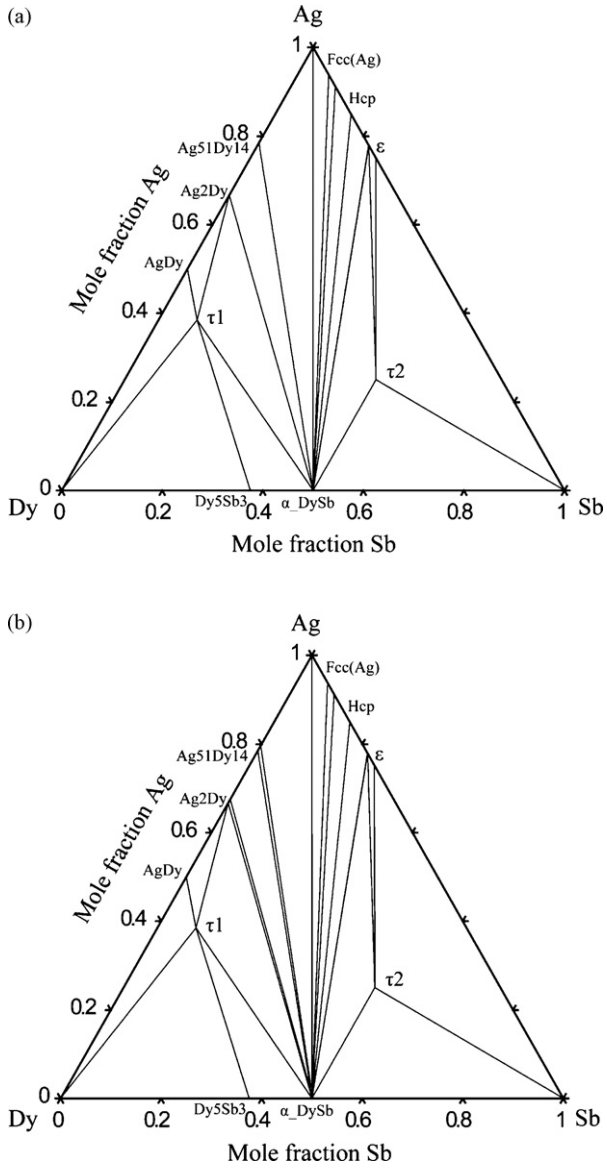

Fig. 5. The calculated (a) and experimental (b) [7] isothermal section of the Ag–Dy–Sb ternary system at 673 K.

in the Dy–Sb system are listed in Table 2. It is easy to see that most experimental data for the diagram boundaries were well reproduced. The differences between the calculated and measured temperatures of all invariant equilibria are less than 8 K. Although at the Sb-rich side, the calculated liquidus curve slightly deviates from the experimental data, the assessed results in present work can still be accepted considering the experimental errors. As pointed out by Mironov et al. [3], due to the high volatility of Sb at high temperature, it is difficult to obtain reliable liquidus in the region with more than 50 at.% Sb. Because the composition of the sample may shift to Dy-rich side during heating compared to the normal one, the liquidus curves shift to Dy-rich side. Obviously, this deviation should decrease with decreasing the content of Sb.

Formation enthalpies of the compounds at 300 K were calculated in comparison with the experimental data as illustrated in Fig. 4. Apparently, the calculated values agree with the experimental data with reasonable deviations.

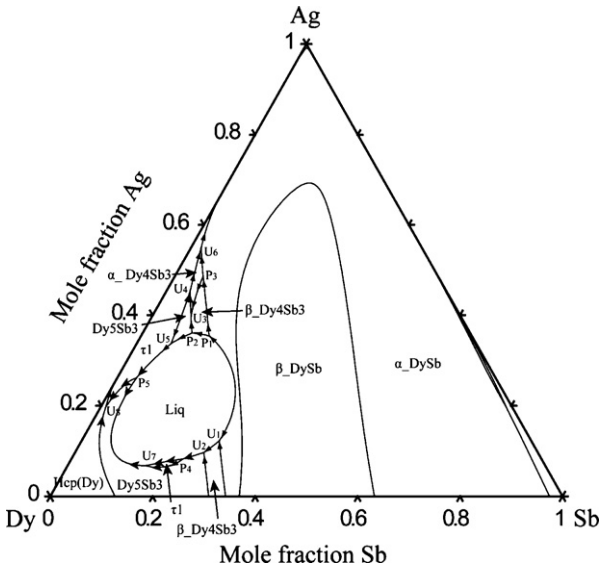

Fig. 6. The calculated liquidus projection of the Ag–Dy–Sb ternary system.

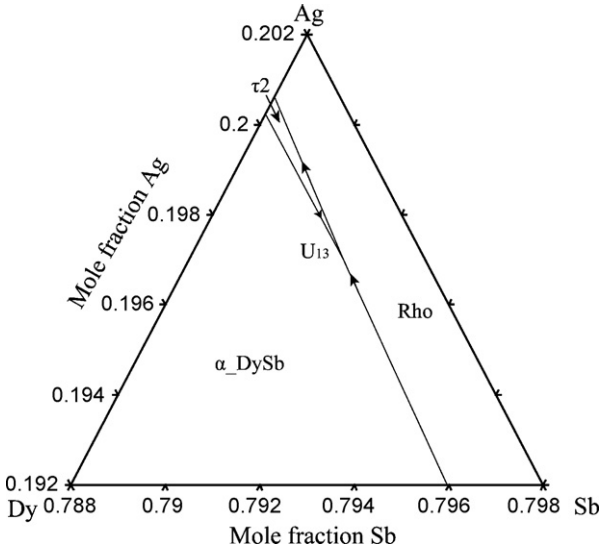

Fig. 7. Enlarged part of the liquidus projection in the Ag–Dy–Sb ternary system.

4.2. The Ag–Dy–Sb ternary system

By using the presently optimized parameters of the Dy–Sb system along with the reported parameters of the Ag–Dy and Ag–Sb [10] systems, and based on the ternary phase relations proposed by Zeng and Xie [7], phase equilibria in the Ag–Dy–Sb ternary system has been further extrapolated. The thermodynamic parameters are listed in Table 1. The calculated and experimental Ag–Dy–Sb isothermal sections at 673 K are shown in Fig. 5. It is easy to see that the stability of the compounds Ag_5Dy_7Sb and $AgDySb_2$, and all the other experimental phase relations have been well reproduced.

Additionally, the liquidus projection is calculated as shown in Figs. 6 and 7. Invariant reactions E_1, E_2, E_3, U_9 and U_{10} are very close to the Ag–Dy binary subsystem, and E_4, U_{11}, U_{12}, U_{13} and U_{14} are very near to the Ag–Sb binary subsystem, so, these 10 invariant reactions cannot be visible in Fig. 6. The calculated invariant reactions and temperatures involved liquid in the Ag–Dy–Sb ternary system are summarized in Table 3. Further experimental information is needed to verify the liquidus projection.

Table 3
Calculated invariant reactions and temperatures of the Ag–Dy–Sb ternary system.

Type	Reaction	T (K)
E_1	$L \leftrightarrow \tau_1 + Ag_2Dy + AgDy$	1222.5
E_2	$L \leftrightarrow \alpha\_DySb + Ag_2Dy + Ag_{51}Dy_{14}$	1182.1
E_3	$L \leftrightarrow \alpha\_DySb + Ag_{51}Dy_{14} + Fcc(Ag)$	1074.8
E_4	$L \leftrightarrow \tau_2 + Rho + \varepsilon$	753.2
U_1	$L + \alpha\_DySb \leftrightarrow \beta\_Dy_4Sb_3 + L$	2002.8
U_2	$L + \beta\_Dy_4Sb_3 \leftrightarrow L + Dy_5Sb_3$	1917.8
U_3	$L + \beta\_Dy_4Sb_3 \leftrightarrow Dy_5Sb_3 + \alpha\_Dy_4Sb_3$	1903
U_4	$L + Dy_5Sb_3 \leftrightarrow \tau_1 + \alpha\_Dy_4Sb_3$	1851
U_5	$L + Dy_5Sb_3 \leftrightarrow \tau_1 + L$	1830.6
U_6	$L + \alpha\_Dy_4Sb_3 \leftrightarrow \tau_1 + \alpha\_DySb$	1752.4
U_7	$L + \tau_1 \leftrightarrow L + Dy_5Sb_3$	1630.1
U_8	$L + Dy_5Sb_3 \leftrightarrow \tau_1 + Hcp(Dy)$	1372.4
U_9	$L + \alpha\_DySb \leftrightarrow \tau_1 + Ag_2Dy$	1245
U_{10}	$L + \tau_1 \leftrightarrow AgDy + Hcp(Dy)$	1171.2
U_{11}	$L + Fcc(Ag) \leftrightarrow \alpha\_DySb + Hcp(Dy)$	974.4
U_{12}	$L + Hcp(Dy) \leftrightarrow \alpha\_DySb + \varepsilon$	835.5
U_{13}	$L + \alpha\_DySb \leftrightarrow \tau_2 + Rho$	831
U_{14}	$L + \alpha\_DySb \leftrightarrow \tau_2 + \varepsilon$	818.1
P_1	$L + \alpha\_DySb \leftrightarrow \beta\_Dy_4Sb_3$	2002.8
P_2	$L + \beta\_Dy_4Sb_3 \leftrightarrow Dy_5Sb_3$	1917.8
P_3	$L + \beta\_Dy_4Sb_3 + \alpha\_DySb \leftrightarrow \alpha\_Dy_4Sb_3$	1903
P_4	$L + Dy_5Sb_3 \leftrightarrow \tau_1$	1830.6
P_5	$L + \tau_1 \leftrightarrow Dy_5Sb_3$	1630.1

5. Conclusion

With the CALPHAD method, the Dy–Sb binary system was optimized, and thermodynamic description of the Ag–Dy–Sb ternary system has been performed. Good agreement between the calculated and experimental data has been realized and a set of thermodynamic parameters for describing the Ag–Dy–Sb ternary system have been obtained.

Acknowledgements

This work was financially supported by the National Natural Science Foundation of China (No. 50671122) and Hunan Provincial Innovation Foundation for Postgraduate (No. 1343–74236000007). The optimization was carried out by using the Thermo_Calc program licensed from Thermo_Calc Software AB, Stockholm, Sweden. Partial calculations were performed using the Pandat program licensed from The Compu Thermo, LLC, Madison, WI, USA.

References

[1] J.Z. Wang, K. Gao, Z.J. Chen, J. Chin. Rare Earth Soc. 14 (1995) 488–497.
[2] Y.T. Ning, Precious Met. 15 (1994) 61–71.
[3] K.E. Mironov, M.N. Abdusalyamova, O.R. Burnashev, Inorg. Mater. 16 (1980) 1332–1336.
[4] A.V. Morozkin, J. Alloys Compd. 358 (2003) L6–L8.
[5] A.V. Morozkin, I.A. Sviridov, A.V. Leonov, J. Alloys Compd. 335 (2002) 139–141.
[6] L.M. Zeng, J.J. He, J.L. Yan, W. He, J. Alloys Compd. 479 (2009) 173–179.
[7] L.M. Zeng, X.Y. Xie, J. Alloys Compd. 365 (2004) 178–180.
[8] R. Ferro, G. Borzone, G. Cacciamani, Thermochim. Acta 129 (1988) 99–113.
[9] B.Z. Lee, C.S. Oh, D.N. Lee, J. Alloys Compd. 215 (1994) 293–301.
[10] C.S. Oh, J.H. Shim, B.J. Lee, D.N. Lee, J. Alloys Compd. 238 (1996) 155–166.
[11] A.T. Dinsdale, CALPHAD 15 (1991) 317–425.